Interpreting the deformation phenomena of a levee damaged during the 2012 Emilia earthquake

Anna Chiaradonna, Anna d'Onofrio & Francesco Silvestri
Department of Civil, Architectural and Environmental Engineering – University of Naples Federico II, Naples, Italy
Giuseppe Tropeano
Department of Civil, Environmental Engineering and Architecture – University of Cagliari, Cagliari, Italy

ABSTRACT
The seismic sequence in May 2012 that struck a large area of the river Po Valley (Emilia-Romagna region, Northern Italy) triggered significant fractures, deformations, and liquefaction occurrences in a number of riverbanks located close to the earthquake epicenter. Among them, one of the most severely damaged structures turned out to be the levee of an irrigation canal flowing through a small village near the historic town of Ferrara (Italy). Large, longitudinally-oriented ground cracks were observed along a 3 km bank stretch, causing in turn severe structural damages to approximately one hundred houses and productive activities built on the bank crown.

An extensive study, including in-situ and laboratory investigation, was carried out in order to identify possible damage causes as well as to suggest seismic risk mitigation actions. The significant depth of the seismic bedrock required a detailed definition of the geotechnical subsoil model and of the actual input motion on rigid bedrock.

Slope stability and liquefaction susceptibility analyses of the embankment were carried out adopting approaches with an increasing level of complexity. Effective stress analysis on a reference soil column highlighted some criticisms on the foundation soils of the dyke, allowing to better understand the seismic behaviour of the levee during the Emilia 2012 earthquake.

1 INTRODUCTION

On May 20, 2012 an earthquake of magnitude M_L = 5.9 struck northern Italy, caused severe damage on a large area of the river Po Valley, in the Emilia-Romagna region (Figure 1). From a scientific point of view, the seismic event represented an important case study due to the location of the damaged sites in a deep basin structure as well as to the extensive occurrence of soil liquefaction unusual in the Italian context (Fioravante et al., 2013).

Indeed, the hit area is located in the south of the Po plain, in the foreland basin of two mountain chains constituted by the Alps and the northern Appennine. A complex system of tectonic structures is buried under a thick sedimentary fill, so that the thrusts are generally buried (Fioravante et al., 2013). The main tectonic structure is a buried ridge, known as Ferrara folds, which reaches its maximum height, about 120 m below the ground surface, near the city of Ferrara (Tonni et al., 2015).

The subsoil is characterized by alluvial deposits of different depositional environments, which consist of alternating layers of silty-clayey deposits and sandy soils mainly constituting ancient rivers banks. Most of the liquefaction evidences were observed along abandoned old canals and active inhabited levees. As a matter of fact, more than 20 km of levees were damaged with an estimated economic loss of more than 40 million euros. One of the most damaged sites was an embankment along an irrigation canal known as Canale Diversivo di Burana, flowing through the small village of Scortichino, in the Municipality of Bondeno (Figure 1).

An extensive study, including in-situ and laboratory investigation, was carried out in order to identify possible damage causes as well as to suggest seismic risk mitigation actions. Simplified liquefaction assessments of the embankment, carried out adopting different empirical approaches gave rise to contradicting results. For this reason, the susceptibility analysis was carried out adopting approaches with a higher level of complexity (Tonni et al., 2015).

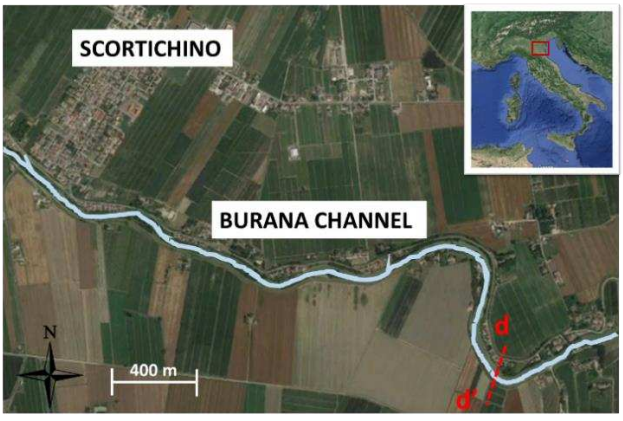

Figure 1. Scortichino bank stretch and location of the studied section d-d'.

Here, the results of an effective stress analysis carried out on a reference soil column of the dyke to simulate the seismic response of potentially liquefiable soils during the strong shaking, are presented.

After a detailed definition of the geotechnical subsoil model at the site, the actual input motion at the rigid bedrock was obtained by deconvolving the ground motion recorded at the surface at a nearby station. Effective stress analysis was then carried out by adopting the code SCOSSA (Tropeano et al., 2016).

Analysis results highlighted some criticisms at the foundation soil of the dyke, allowing to better understand the seismic behaviour of the levee during the Emilia 2012 earthquake.

2 CASE STUDY

The “Canale Diversivo di Burana” was designed in 1884 with a dual aim. During the winter season, the channel collects rainwater from the countryside and several small villages through a dense network of secondary channels and then it delivers the rainwater in the Panaro river. On the contrary, the direction of the water flow is reverse during the summer season when the Burana channel works as an irrigation canal for the surrounding plain. The channel becomes a hanging canal along the Scortichino village, where an embankment was built. Over the centuries, houses and small economic activities settled on the crest of embankment, forming little settlements along the channel where the cross section of the embankment is wider (Figure 1).

After the 2012 Emilia earthquake, large, longitudinally-oriented ground cracks where observed along a 3 km bank stretch, causing in turn severe structural damages to a large part of the approximately one hundred houses and economic activities built on the bank crown. Many of the buildings were affected by a series of failures, such as detachments and rotations of bordering buildings, cracks in walls of houses, and structural damages (Tonni et al., 2015).

In order to evaluate if it was necessary to relocate houses and any economic activities, the Emilia-Romagna regional authority launched an in-depth study aimed at evaluating the response of the dyke during the 2012 earthquake sequence and identifying possible damage causes and relevant remedial measures. A number of geotechnical investigations were carried out, in-situ and laboratory tests, aimed at defining an accurate geotechnical model. The soil investigation was concentrated around the most damaged cross sections of the dyke (Tonni et al., 2015). The height of the dyke is variable from a minimum of 5 m to a maximum of 8 m at section d-d’, which corresponds also to the widest crest of the dyke (about 55 m). In this study, the analysis results relevant to this section are presented (Figure 1).

The field investigation consists of 5 boreholes reaching 20 to 50 m below the ground surface, during which undisturbed samples were extracted. Two boreholes were equipped with inclinometers up to 20 m depth, while the others were equipped with piezometers. Moreover, penetration tests with piezocone (CPTU) and seismic dilatometer tests (SDMT) were carried out both at the crest of the riverbank and at the toe, up to a depth varying between 25 – 35 m.

Finally, in-situ permeability tests were performed using the Lefranc method at depths of 8 and 15 m.

The laboratory experimental programme included a large variety of geotechnical tests for the determination of both static and dynamic properties of the 29 available samples, such as undrained triaxial tests (TXCU), direct shear tests (DT), cyclic simple shear tests (CSS), double specimen direct simple shear tests (DSDSS), cyclic torsional shear tests (CTS), and resonant column tests (RC). All the details of the extensive field and laboratory investigations as well as the interpretation of the results can be found in Tonni et al. (2015).

3 INPUT MOTION

The main shock of the Emilia 2012 earthquake sequence occurred on May 20, 2012 at 02:03:53 UTC time.

The station of the Italian Strong Motion Network (DPC) located in Mirandola town recorded the strong motion and the subsequent aftershocks. The Mirandola (MRN) station recorded the highest PGA during the mainshock of May 20th, since it is very close to the epicenter (Lat = 44.8782°, Long = 11.0617°) (Figure 2).

The record cannot be used directly as input motion in the analysis, because the station is located on a Class C site, with a $V_{S,30}$ = 208 m/s, according to Eurocode 8 (EC8). As previously mentioned, the 2012 seismic sequence affected an alluvial plain with a significant depth of the seismic bedrock, so that the closest Class A stations are located too far from the epicenter. To overcome this problem, the acceleration record at MRN station (Figure 3a) has been deconvoluted to the bedrock and, finally, the deconvoluted outcrop motion has been scaled to account for the different epicentral distance of the Scortichino site, as it will be detailed in Sec. 3.2.

The EW component of the recorded mainshock has been considered in the following, since it is characterised by the highest PGA value (INGV, 2016).

Figure 2. Fault plane of the mainshock of May, 20th and location of the MRN station (INGV, 2016)

3.1 De-convolution of surface motion

The deconvolution procedure requires the definition of the subsoil model under the recording station. The MRN station is located along the Napoli street in the Mirandola municipality, very close (≈ 100 m) to the site where a

downhole seismic array has been deployed since the earthquake. During the deployment of the array, a cross-hole test was carried out until 125 m depth. Figure 3b illustrates the stratigraphic sequence and the shear wave velocity profile obtained from the cross-hole test. This configuration has been adopted for defining the subsoil model under the recording station. Since no site-specific laboratory data are available, the shear modulus reduction and damping curves were assumed to be the same of the soil deposits at Scortichino (Figure 3d), where they have been measured by resonant column and double specimen direct simple shear tests (Tonni et al., 2015).

Deconvolution consists of assigning a recorded ground motion at the surface of a 1D soil column and using a linear equivalent analysis to calculate the acceleration time history at the bedrock.

For soft sites, Silva (1988) measured the coherence in order to provide an estimate of goodness of fit between the simulated propagated motion and that recorded at the surface. The results show that the coherence between the recorded surface motion and that analytically propagated to surface drops off at the frequency 15 Hz. For this reason, a low pass (LP) filter at 15 Hz has been applied to the recorded surface motion to be used for the deconvolution analysis. Moreover, from the coherence analysis it appears that the maximum energy that is propagated as normally incident shear waves is about 75%. The remaining energy may be due to scattered waves and perhaps to P-waves. This has significant implications on the non-linear behaviour of the soils.

In particular, attempting to deconvolute the total surface motion as vertically propagating shear waves may result in too much energy predicted at depth, leading to excessive estimates of modulus-reduction and mobilised damping. The overall effect is the overestimation of the motion at depth that is required to produce the total observed surface motion (Silva, 1988).

The guidelines for equivalent-linear de-convolution proposed by Silva (1988) were summarised by Markham et al. (2015) in the following steps:

1) a low pass (LP) filter was applied to the recorded surface motion to be used for the de-convolution analysis at 15 Hz and scaled by 0.87; SeismoSignal was used to perform a 4th order, LP Butterworth filter;
2) the filtered and scaled motion from step 1 was assigned as input motion at the surface of a 1D soil column;
3) the motion from a layer of interest at some depth below the surface is obtained via an equivalent linear solution;
4) the final iteration values of shear modulus reduction and material damping for each layer during the de-convolution process are obtained;
5) the deconvolution process was performed again by using a linear analysis with the final values of normalized stiffness, G/G_0, and equivalent damping, D, from step 4 for each layer of the 1D soil column and introducing the LP filtered (15 Hz) full surface motion (i.e. not scaled by 0.87) at the top of the column to obtain the "final", outcropping, deconvoluted motion.

In this study, the EERA (Bardet et al., 2000) code was utilized to perform all deconvolution analyses. The deconvoluted outcrop input motion is shown in Figure 3c.

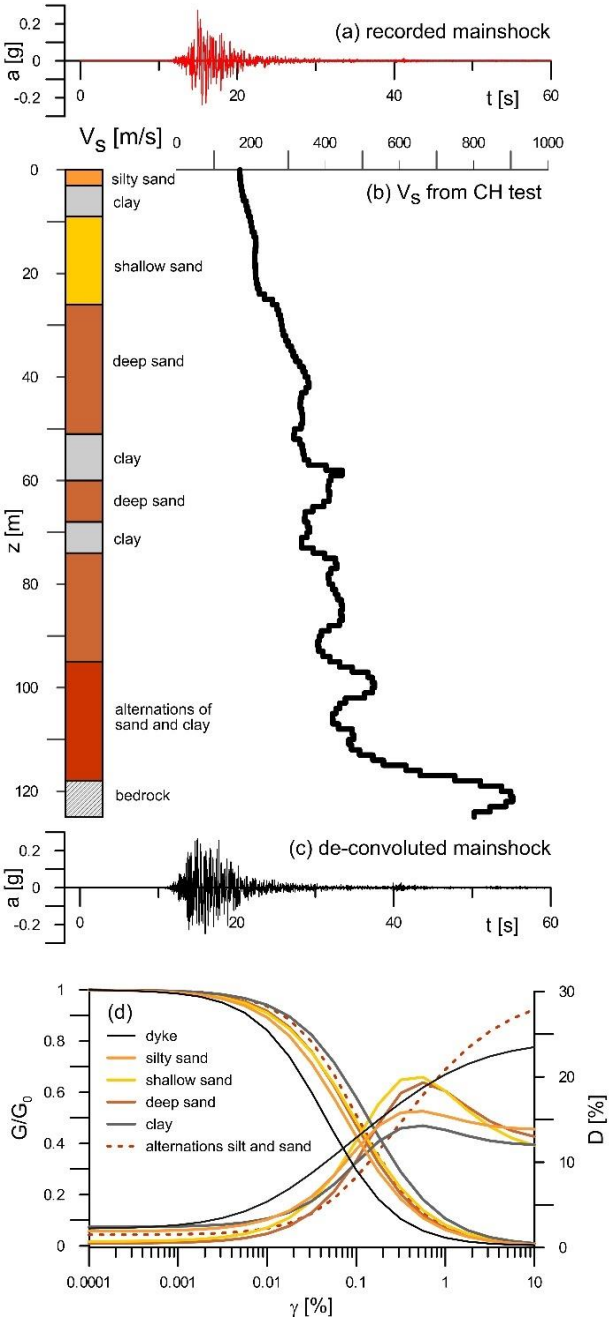

Figure 3. (a) Subsoil model for de-convolution analysis (d) Stiffness and damping vs strain

3.2 Attenuation law

Due to the great difference in distance from the epicenter of the MRN station and of the dyke site (Figure 2), a study of ground motion attenuation has been necessary. This consists essentially of predicting ground motion at a particular site by means of attenuation laws, formulated on the basis of large strong motion databases and depending on soil type and faulting mechanism.

Similarly to Sinatra and Foti (2015), a ground motion prediction equation (GMPE) based on the Italian strong motion database has been adopted (Bindi et al., 2011). The GMPE for peak ground acceleration (PGA, cm/s^2) is:

$$\log(\text{PGA}) = e_1 + F_D(R,M) + F_M(M) + F_S + F_{sof} \quad [1]$$

where e_1 is a constant term equal to 3.672, $F_D(R, M)$, $F_M(M)$, F_S and F_{sof} are the distance function, the magnitude scaling, the site amplification and the style of faulting correction, respectively. M is the moment magnitude, M_w, and R is the Joyner-Boore distance, R_{jb}. The proposed equation for the distance function is:

$$F_D(R,M) = \left[c_1 + c_2\left(M - M_{ref}\right)\right]\log\left(\frac{\sqrt{R^2+h^2}}{R_{ref}}\right) + c_3\left(\sqrt{R^2+h^2} - R_{ref}\right) \quad [2]$$

while the magnitude function is:

$$F_M(M) = \begin{cases} b_1\left(M - M_h\right) + b_2\left(M - M_h\right)^2 & \text{for M} \le M_h \\ b_3\left(M - M_h\right) & \text{otherwise} \end{cases} \quad [3]$$

The numerical values of the constants for the estimation of peak ground acceleration are reported in Table 1.

The functional form F_S in equation 1 represents the site amplification and it is given by:

$$F_S = s_j \cdot C_j \quad \text{for } j = 1, \ldots, 5 \quad [4]$$

where C_j are dummy variables used to denote the five different EC8 site classes from A to E.

In the same way, the functional form F_{sof} represents the type of faulting correction and it is given by:

$$F_{sof} = f_j \cdot E_j \quad \text{for } j = 1, \ldots, 4 \quad [5]$$

where E_j are dummy variables used to check the fault type: normal, reverse, strike-slip, and unknown.

Bindi et al. (2011) show the numerical values of the s_j and f_j coefficients.

For the mainshock of the Emilia earthquake (M_w = 6.1), the fault mechanism is reverse type and the subsoil site class is C, as reported in ITACA database (Luzi et al., 2016). Site and style of faulting coefficients adopted in the GMPE for horizontal PGA are also reported in Table 1.

The fault projection on the ground surface allows for computing the Joyner-Boore distance of the MRN station, R_{jb} = 4.34 km. The Scortichino dyke is located inside the surface projection of the fault (R_{jb} = 0.1 km as default value), and an amplification of the recorded motion at the MRN station is expected (Figure 2).

Figure 4 shows the attenuation law of the mainshock in blue lines, using the input parameters in Table 1. The same plot shows also PGA of the de-convoluted outcrop motions of the shock (red point). The GMPE was scaled to the PGA of the de-convoluted motion. The latter has been used to define the values of PGA expected at the site of Scortichino. Finally, the de-convoluted motion was scaled to so-computed peak acceleration value of 0.344 g.

Table 1. Constants and Coefficients for GMPE (Bindi et al., 2011).

Coefficient	Value	Coefficient	Value
c_1	-1.940	M_h	6.75
c_2	0.413	R_{ref} (km)	1
h	10.322	s_C	0.240
c_3	$-1.34\cdot10^{-4}$	f_2	$1.05\cdot10^{-1}$
b_1	-0.262	σ_B	0.172
b_2	-0.0707	σ_W	0.290
M_{ref}	5	σ	0.337

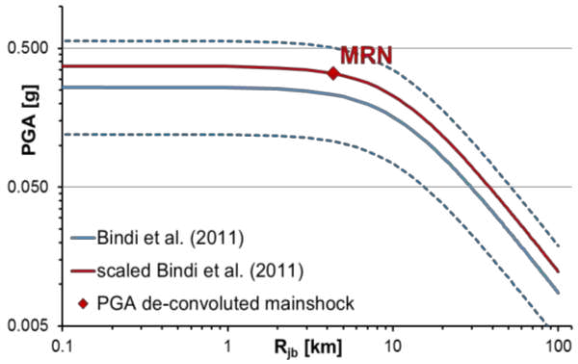

Figure 4. Ground motion attenuation law

4 GEOTECHNICAL MODEL AND PRELIMINARY ANALYSES

Figure 5 shows the considered cross section of the dyke as obtained by analyzing the results of boreholes and field tests. The core of the dike and its foundation soil consist of a silty sand, which rests upon a thick layer of alluvial sands, interbedded by clay.

Seepage analysis with the code SEEP/W (Geostudio, 2007) was used to simulate the ground water level within the embankment section, consistent with the piezometric measurements performed within the deep sands (Figure 5).

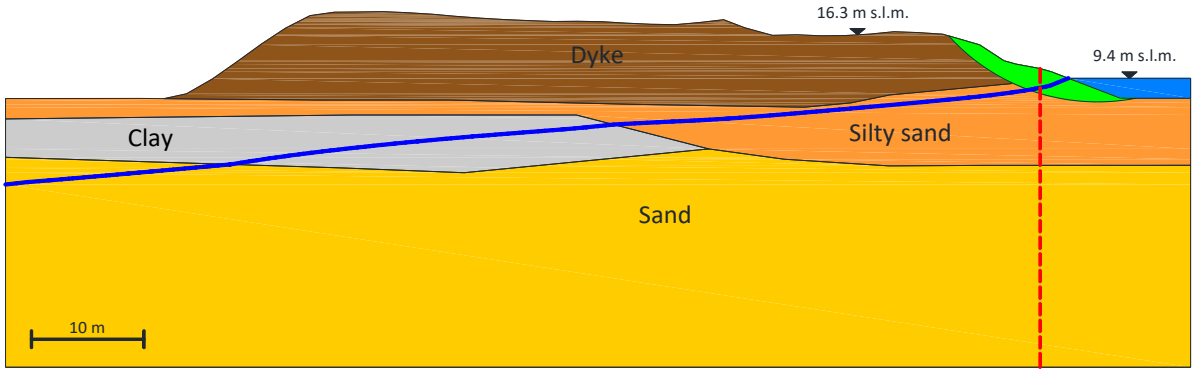

Figure 5. Stratigraphic model of the cross section d - d' with critical sliding surface and reference soil column in red

Due to the high degree of saturation of the undisturbed samples (> 95%), taken at a shallow depth from the ground surface, the seepage analysis was carried out using the saturated permeability of soils.

Hydraulic conductivity of the soils has been measured from field investigations, both directly from Lefranc tests and indirectly evaluated using empirical correlations (Table 2).

The boundary conditions of the seepage analysis are constituted by the level of water table in the channel and the hydrostatic condition along the perimeter of the section. The ground water at 7.7 m below the ground surface was applied along the vertical land side of the domain, as indicated by the piezometric measures (Tonni et al., 2015).

The seepage analysis yielded the piezometric surface inside the embankment shown in Figure 5 with a blue line. As a consequence, the slope stability of the riverside of the dyke appeared to be strongly reduced by the increase of the pore pressure build-up in seismic condition (Tonni et al., 2015).

For evaluating the slope stability of the riverside of the dyke, the yield acceleration of 0.175 g was computed adopting the Morgenstern-Price (1965) method. The pseudo-static analyses and the related critical sliding surface are reported in Figure 5. Material parameters assumed for the different stratigraphic units are reported in Table 2.

In order to define an equivalent acceleration time history at the depth of the sliding surface, a seismic site response analysis in effective stress condition was performed on a soil column assumed as reference of the seismic behaviour of the dyke.

Table 2. Properties of the soil deposits.

Soil deposits	Permeability coefficient (m/s)	Friction angle (°)	coefficient of pressure at rest	Poisson ratio
dyke	$1 \cdot 10^{-6}$	33	0.44	0.306
silty sand	$1 \cdot 10^{-6}$	33	0.44	0.306
clay	$1 \cdot 10^{-8}$	25.5	0.59	0.371
sand	$3 \cdot 10^{-5}$	38	0.4	0.286

According to the criterion suggested by Blake et al. (2002), the soil profile considered for the analyses is that corresponding to the maximum depth of the critical sliding surface (red dashed line in Figure 5). The adopted one-dimensional model included the bedrock at 115 m depth (Figure 7a), based on geologic studies that reconstructed the rigid bedrock depth at 120 m under the crest of the embankment (Tonni et al., 2015).

To perform dynamic analyses, the shear wave velocity profile (Figure 7b) was defined by integrating the results of the SDMTs with the measurements of two Cross-Hole tests carried out in the towns of Mirandola and Medolla, which reached 130 m depth (Laurenzano and Priolo, 2013). The borehole related to the Cross-Hole tests made possible to reconstruct the stratigraphic sequence at Scortichino over 50 m deep. The deepest stratigraphy essentially consists of a thick sand layer resting on an alternation of centimetric layers of sands and silts (Figure 7a).

The normalized shear modulus and damping ratio curves adopted to simulate the non-linear soil behaviour of the soil deposits were the same as those presented in Figure 3c. The shear modulus reduction curves were analytically fitted using the modified Konder and Zelasko (1963) model according to the procedure for strength compatibility proposed by Gingery and Elgamal (2013), in order to better match the soil behaviour at large strains up to failure (Chiaradonna et al., 2015).

Excess pore water pressure build-up in the saturated soils has been modelled with a simplified model based on the accumulation of shear stress (Chiaradonna et al., 2016). It permits comparison of irregular time-history of shear stress induced by earthquake with the soil liquefaction resistance, evaluated in stress-controlled cyclic laboratory tests.

Figure 6 shows the experimental results of cyclic simple shear tests taken on soil samples of silty sand and sand layers (Tonni et al., 2015). The number of cycles to liquefaction, N_L, was established assuming that liquefaction occurs at a pore pressure ratio (excess pore pressure normalized by the initial effective confining pressure) $r_u = 0.90$.

The model adopted in this study describes the cyclic resistance curve as follows (Figure 6a):

$$\frac{(SR - SR_t)}{(SR_r - SR_t)} = \left(\frac{15}{N}\right)^{\frac{1}{\alpha}} \quad [6]$$

where SR is the shear stress amplitude normalized by the initial effective confining pressure; N is the number of cycles, SR_r is the ordinate of the curve for N = 15 (usually adopted as a reference number of cycles). The parameters α and SR_t respectively describe the steepness and the horizontal asymptote of the curve.

Since the threshold value, SR_t, of the cyclic resistance curve was not clearly defined by the experimental data; it was estimated from the backbone curve as that corresponding to the volumetric threshold strain measured in resonant column tests (Chiaradonna et al., 2015). The parameter α was finally determined as the slope of the cyclic resistance curve.

Moreover, the pore pressure model expresses the pore pressure ratio, r_u, as a function of the normalized number of cycles, N/N_L (Figure 6b):

$$r_u = a\left(\frac{N}{N_L}\right)^b + c\left(\frac{N}{N_L}\right)^4 \quad [7]$$

where a, b and c are curve-fitting parameters. The pore pressure parameters calibrated for the two sandy soil deposits are reported in Table 3.

Table 3. Pore pressure parameters of the soil deposits.

Soil deposits	α	SR_t	SR_r	a	b	c
silty sand	1.85	0.078	0.18	0.81	0.54	0.09
sand	1.97	0.08	0.16	0.54	0.50	0.36

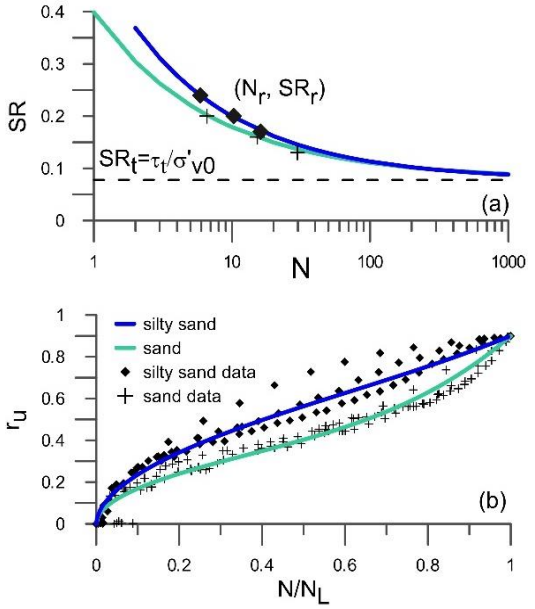

Figure 6. Cyclic resistance curves (a) related pore water pressure relationship (b) for clean sand and silty sand

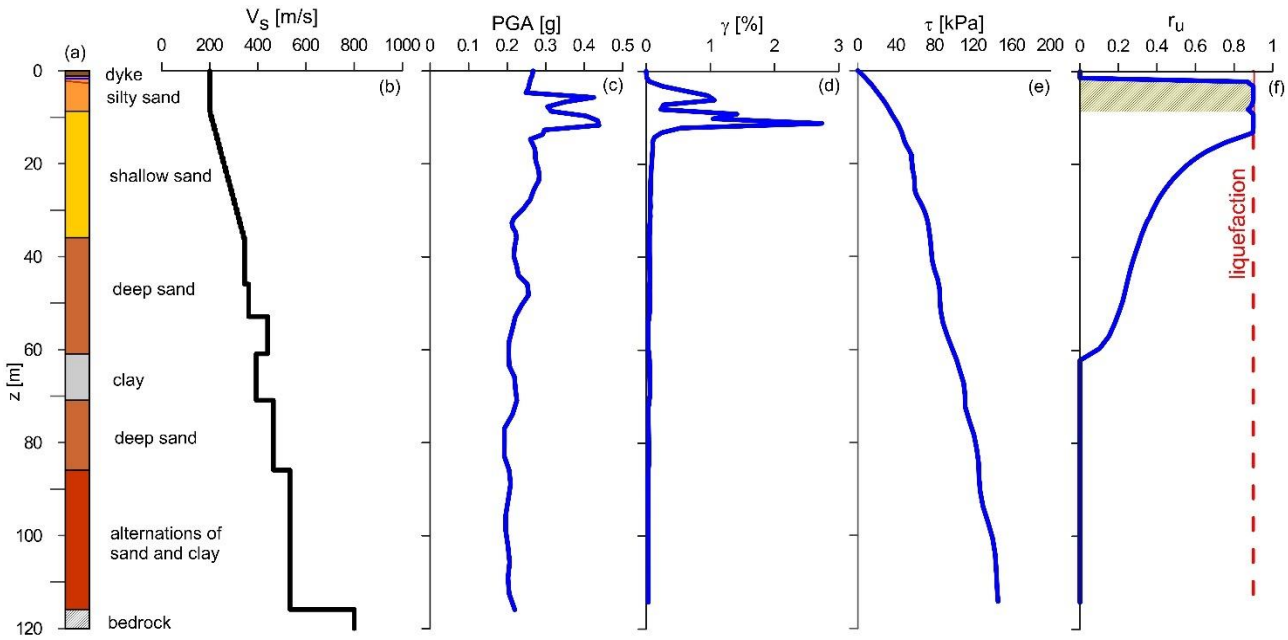

Figure 7. Effective stress analysis with dissipation on d – d' section for the deconvoluted main shock. a) subsoil profile; b) shear wave velocity and envelope of: c) maximum acceleration; d) maximum shear strain; e) maximum shear stress and f) maximum pore pressure ratio.

Due to the lack of the shallow clay layer in the soil column, the dissipation and redistribution of pore pressure, modelled using the one-dimensional theory of consolidation, were also taken into account in the analysis.

The ground level and the bedrock surface were assumed to be drainage surfaces, since the bedrock is constituted by a fractured calcareous rock. The consolidation coefficients were defined as a function of permeability and of the constrained modulus, E_{oed}, expressed as follows:

$$E_{oed} = \frac{2G_0 \cdot (1-\nu)}{(1-2\nu)} \quad [8]$$

where ν is the Poisson ratio computed from the coefficient of pressure at rest, measured during the SDMT tests (Table 2).

The build-up and dissipation models were incorporated in a program for 1D seismic response analyses in the time domain, SCOSSA (Tropeano et al., 2016), in order to carry out coupled dynamic analyses in terms of effective stress.

5 EFFECTIVE STRESS ANALYSIS RESULTS AND DISPLACEMENTS EVALUATION

Figure 7c-f reports the results of the analysis in terms of maximum envelope profiles of acceleration, shear strain, shear stress and pore pressure ratio.

Liquefaction was reached between 3 and 12 m below the ground surface, within the silty sand layer and the shallowest part of the sand deposit.

The acceleration profile is characterized by a significant reduction between the surface and the foundation soils of the dyke; this effect can be attributed to the liquefied/degraded soil layer, which work as dampers against the motion.

Maximum shear strains were reached at about 12 m under the ground level, due to the accumulation of plastic strains in the $\tau - \gamma$ cycles of the liquefiable soils.

Figure 7f also highlights the thickness of the liquefiable soil resulted from the simplified liquefaction analysis based on the CPTU tests reported in Tonni et al. (2015) (hatched grey area). It is mainly constituted by the silty sand deposit under the dyke.

Figure 8a shows the time history of shear stress and excess pore pressure at the depth of the critical sliding surface, which is located in the silty sand layer (i.e. 2.2 m under the surface of the reference soil column). Every time the shear stress overcomes the threshold values, τ_t, excess pore pressure is generated. Since the sliding surface is very close to the drainage surface, the consolidation curve is well-defined. It can be noted that the dissipation process started after the most critical stage of the time history (~16 s) and it continued after the end of the seismic shaking. Finally, a Newmark displacement analysis was performed considering the equivalent accelerogram at the depth of the critical sliding surface.

The equivalent accelerogram, $a_{eq}(t)$, was computed from the dynamic simulation as the ratio between the shear stress time history at the depth of the sliding surface, $\tau(t,\ z = 2.2\ \text{m})$, and the vertical stress at the bottom of the unstable mass, $\sigma_v(z = 2.2\ \text{m})$, as follows:

$$a_{eq}(t) = \frac{\tau(t, z = 2.2\text{m})}{\sigma_v(z = 2.2\text{m})} \text{g} \quad [9]$$

Figure 8b shows the result of the displacements analysis. Accumulation of displacements occurs when acceleration overcomes the yield acceleration, a_y.

The final accumulated displacement is1.6 cm, which is compatible with the width of the cracks observed along the dyke.

6 CONCLUSION

Approaches with an increasing level of complexity have been applied in order to simulate the seismic response of a river bank damaged during the 2012 Emilia earthquake.

A seismic site response analysis in terms of effective stress has been performed on a soil column, assumed as representative of the seismic behaviour of the riverside slope of the dyke.

The results showed that liquefaction occurred within the silty sand and shallowest sandy layers of the dyke, even though significant excess pore pressures appear until 20 m under the surface in the sand deposit.

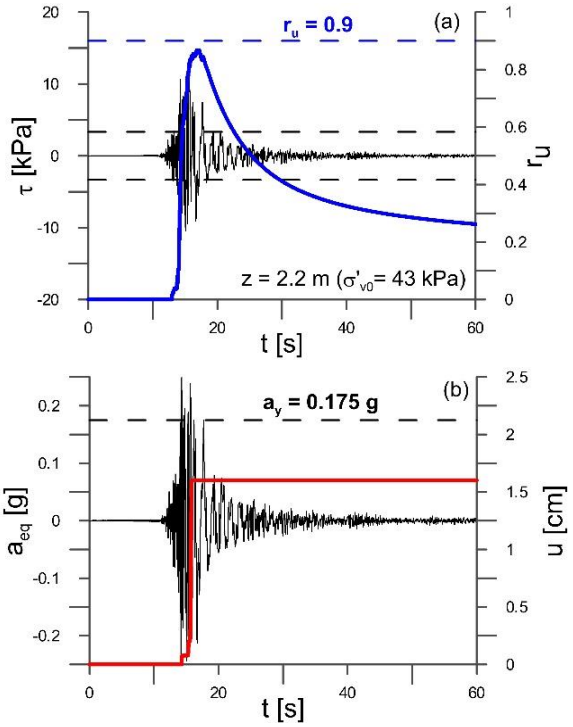

Figure 8. (a) Shear stress and excess pore pressure ratio and (b) equivalent acceleration and displacement time histories at the depth of the critical sliding surface (2.2 m depth) for the reference soil column

The results of the simulation appear to be consistent with some of the preliminary liquefaction analysis carried out by Tonni et al. (2015) and the computed displacements are compatible with the observed damage.

7 REFERENCES

Bardet, J.P., Ichii, K. and Lin, C.H. 2000. EERA – A computer program for equivalent-linear earthquake site response analyses of layered soil deposits. University of Southern California.

Blake, T.F., Hollingsworth, R.A. and Stewart, J.P. 2002. Recommended Procedures for Implementation of DMG Special Publication 117 Guidelines for Analyzing and Mitigating Landslide Hazards in California. Los Angeles, CA, USA.

Bindi, D., Pacor, F. Luzi, L. Puglia, R. Massa, M. Ameri, G. and Paolucci, R. 2011. Ground motion prediction equations derived from the Italian strong motion database. *Bulletin of Earthquake Engineering*, 9(6): 1899–1920.

Chiaradonna, A., Tropeano, G. d'Onofrio, A. and Silvestri, F. 2015. Application of a simplified model for the prediction of pore pressure build-up in sandy soils subjected to seismic loading. Proc. 6th Int. Conf. Earthquake Geotechnical Engineering, Christchurch, New Zealand.

Chiaradonna, A., Tropeano, G. d'Onofrio, A. and Silvestri, F. 2016. A simplified method for pore pressure buildup prediction: from laboratory cyclic tests to the 1D soil response analysis in effective stress conditions. Proceedings of the VI Italian Conference of Researchers In Geotechnical Engineering, Bologna, Italy.

Fioravante, V., Giretti, D., Abate, G., Aversa, S., Boldini, D., Capilleri, P.P., Cavallaro, A., Chamlagain, D., Crespellani, T., Dezi, F., Facciorusso, J., Ghinelli, A., Grasso, S., Lanzo, G., Madiai, C., Massimino, M.R., Maugeri, M., Pagliaroli, A., Rainieri, C., Tropeano, G., Santucci De Magistris, F., Sica, S., Silvestri, F., Vannucchi, G. 2013. Earthquake geotechnical engineering aspects of the 2012 Emilia-Romagna earthquake (Italy). Proceedings of the 7th international conference on case histories in geotechnical engineering, Chicago, Illinois, USA.

Geostudio 2007. SLOPE/W User's manual. Calgary, Alberta, Canada.

Gingery, J.R., and Elgamal A. 2013. Shear stress-strain curves based on the G/Gmax logic: A procedure for strength compatibility. The 2nd International Conference on Geotechnical and Earthquake Engineering, Chengdu, China.

Kondner, R.L., and Zelasko, J.S. 1963. Hyperbolic stress-strain formulation of sands. In Proceedings of the 2nd Panamerican Conference on Soil Mechanics and Foundation Engineering, Sao Paulo, Brazil. Associação Brasileira de Mecânica dos Solos, 1: 289-324.

Laurenzano, G. and Priolo, E. 2013. Studio sismologico per la caratterizzazione della risposta sismica di sito ai fini della microzonazione sismica di alcuni comuni della Regione Emilia-Romagna, Relazione sull'attività svolta. Istituto Nazionale di Oceanografia e di Geofisica Sperimentale (in Italian).

Luzi, L., Pacor, F. and Puglia, R. 2016. Italian Accelerometric Archive v2.1. Istituto Nazionale di Geofisica e Vulcanologia, Dipartimento della Protezione Civile Nazionale. doi: 10.13127/ITACA/2.1, web: http://itaca.mi.ingv.it/ItacaNet/

Morgenstern, N.R. and Price, V.E. 1965. The Analysis of the Stability of General Slip Surfaces. *Geotechnique*, 15(1): 79-93.

Markham, C.S., Bray, J.D. and Macedo J. 2015. Deconvolution of surface motions from the Canterbury earthquake sequence for use in nonlinear effective stress site response analyses. Proceedings of the 6th International Conference on Earthquake Geotechnical Engineering, paper 176.

Silva, W. 1988. Soil response to earthquake ground motion. Research project 2556-7, Final report prepared by Woodward-Clyde Consultants.

Sinatra, L. and Foti, S. 2015. The role of aftershocks in the liquefaction phenomena caused by the Emilia 2012 seismic sequence. *Soil Dynamics and Earthquake Engineering*, 75: 234 – 245.

Tonni, L., Gottardi, G., Amoroso, S., Bardotti, R., Bonzi, L., Chiaradonna, A., d'Onofrio, A., Fioravante, V., Ghinelli, A., Giretti, D., Lanzo, G., Madiai, C., Marchi, M., Martelli, L., Monaco, P., Porcino, D., Razzano, R., Rosselli, S., Severi, P., Silvestri, F., Simeoni, L., Vannucchi, G. and Aversa, S. 2015. Interpreting the deformation phenomena triggered by the 2012 Emilia seismic sequence on the Canale Diversivo di Burana banks. *Italian Geotechnical Journal*, 2: 28 - 58 (in Italian).

Tropeano, G., Chiaradonna, A., d'Onofrio, A. and Silvestri F. 2016. An innovative computer code for 1D seismic response analysis including shear strength of soils. *Géotechnique*, 66(2): 95–105.